Available online at www.sciencedirect.com
SCIENCE DIRECT®
Carbohydrate Research 338 (2003) 1299–1308
CARBOHYDRATE RESEARCH
www.elsevier.com/locate/carres

Synthesis and conformational analysis of the repeating units of bacterial spore peptidoglycan

Dina Keglević, Biserka Kojić-Prodić,* Zrinka Banić Tomišić†

Rudjer Bošković Institute, P.O. Box 180, Bijenička 54, HR-10002 Zagreb, Croatia

Received 11 July 2002; accepted 27 September 2002

Abstract

Deprotection of the fully blocked disaccharide allyl *O*-(2-amino-4,6-*O*-benzylidene-3-*O*-[(*R*)-1-carboxyethyl]-2-deoxy-β-D-glucopyranosyl-1′,2-lactam)-(1→4)-2-acetamido-3,6-di-*O*-benzyl-2-deoxy-β-D-glucopyranoside by selective de-O-allylation and parallel removal of the benzylidene and *O*-benzyl groups is described. The resulting β-muramyl lactam-(1→4)-GlcNAc disaccharide is characterised as the per-*O*-acetylated derivative by ^{1}H and ^{13}C NMR spectroscopy and X-ray structure analysis. Conformational analysis about glycosidic bond of repeating units of bacterial spore cortex is based on experimental data and molecular modelling.

Keywords: Bacterial spore cortex repeating unit; Peptidoglycan; *N*-Acetylglucosamine; Muramic acid 1′,2-lactam; Synthesis; NMR; X-ray structure analysis; Molecular modelling; Conformational analysis

1. Introduction

The bacterial spore peptidoglycan, so called spore cortex, has a composition different from that of the bacterial vegetative cell. In the β-(1→4)-linked glycan chains of the former a substantial part of muramic acid residues lack the peptide and *N*-acetyl substituents and instead form an intramolecularly cyclised δ-lactam structure.[1]

We have reported[2,3] the synthesis and conformational analysis of several muramic acid δ-lactams and their 4-*O*-(2-acetamido-2-deoxy-β-D-glucopyranosyl)-substituted derivatives. In a previous paper[4] the synthesis of the fully protected disaccharide **1** involving the muramic acid δ-lactam glycosidically linked to the 4-position of the GlcNAc moiety was described. Herein we wish to report on the deprotection of **1** to the unprotected disaccharide **3** which was characterised as the per-*O*-acetylated derivative: *O*-(4,6-di-*O*-acetyl-2-amino-3-*O*-[(*R*)-1-carboxyethyl]-2-deoxy-β-D-glucopyranosyl-1′,2-lactam)-(1→4)-2-acetamido-1,3,6-tri-*O*-acetyl-2-deoxy-D-glucopyranose (**4**) by NMR and X-ray structure analysis. In addition, conformational analysis of glycosidic bond of two (1→4)-linked disaccharide building blocks of spore cortex, i.e., MurLac-GlcNAc (**3**), GlcNAc-MurLac (**5**), and GlcNAc-MurLac anhydride (**6**)[2–4] was performed in an attempt to conformationally characterise the cortex (Scheme 1).

2. Results and discussion

2.1. Synthesis

Several conditions were examined for the selective O-deprotection of the anomeric centre of **1**. The reaction using tris (triphenylphosphine) rhodium(I) chloride (Wilkinson catalyst)[5] and mercuric ion catalysed hydrolysis[6] allowed the reproducible preparation of the corresponding hemiacetal **2** as an anomeric mixture in 85% yield, after chromatographic purification. ^{1}H NMR spectrum of **2** showed the absence of allyl signals and the presence of the GlcNAc anomeric protons as two doublets (δ 5.17, $J_{1,2}$ 3.6 Hz; δ 4.79, $J_{1,2}$ 8.2 Hz) in a α:β ratio of ~3:1.

* Corresponding author. Fax: +385-1-4680245
E-mail address: kojic@rudjer.irb.hr (B. Kojić-Prodić).
† Present address: PLIVA, Pharmaceutical Industry, Incorporated, Research Division, Prilaz baruna Filipovića 25, HR-10000 Zagreb, Croatia.

0008-6215/03/$ - see front matter
doi:10.1016/S0008-6215(03)00067-3

Simultaneous removal of the benzylidene and two benzyl groups was achieved by catalytic hydrogenolysis over 10% Pd/C with (9:1) MeOH–AcOH as the solvent to give the unprotected disaccharide **3** (72%) as a hygroscopic amorphous mass. The ^{1}H NMR spectrum of **3** in D_2O revealed three anomeric signals at δ 5.07, 4.81 and 4.61 with coupling constants J 2, 8, and 8 Hz that were assigned to the α and β forms of the reducing GlcNAc and the β form of the β-(1→4)-linked muramyl-lactam, respectively.

Acetylation of the unprotected disaccharide **3**, followed by silica gel chromatography, afforded (74%) the per-*O*-acetylated derivative **4** as an amorphous mass; attempts to resolve the anomers either by silica gel chromatography or crystallisation were not successful. Full assignement of the ^{1}H and ^{13}C NMR spectra of **4** (Table 1) was achieved by ^{1}H–^{1}H COSY, ^{1}H–^{13}C HETCOR, and HMBC experiments.

In the ^{1}H NMR spectra (1 D, 2 D) of **4** the positions of acetates at C-1, C-3, C-6, C-4′ and C-6′ were confirmed by downfield location of the corresponding H-signals. The ^{13}C NMR spectrum contained signals for three anomeric carbons (90.5, 92.5 and 99.8 ppm) and three carbons (50.8, 52.6 and 56.6 ppm) bearing nitrogen at C-2. The structural assignment was evident from the value of the coupling constant ($J_{1,2}$ 8.0 Hz) of the peracetylated muramyl lactam unit and the chemical shift of H-4 signal (δ 3.89, δ 3.83) of the two anomeric forms of the peracetylated glucosamine residue. The evidence of the Mur Lactam β-(1→4)-GlcNAc linkage in **4** was demonstrated by cross-peaks correlating β-Mur Lactam H-1′ with GlcNAc C-4 and the corresponding β-Mur Lactam C-1′ with the GlcN H-4 resonance.

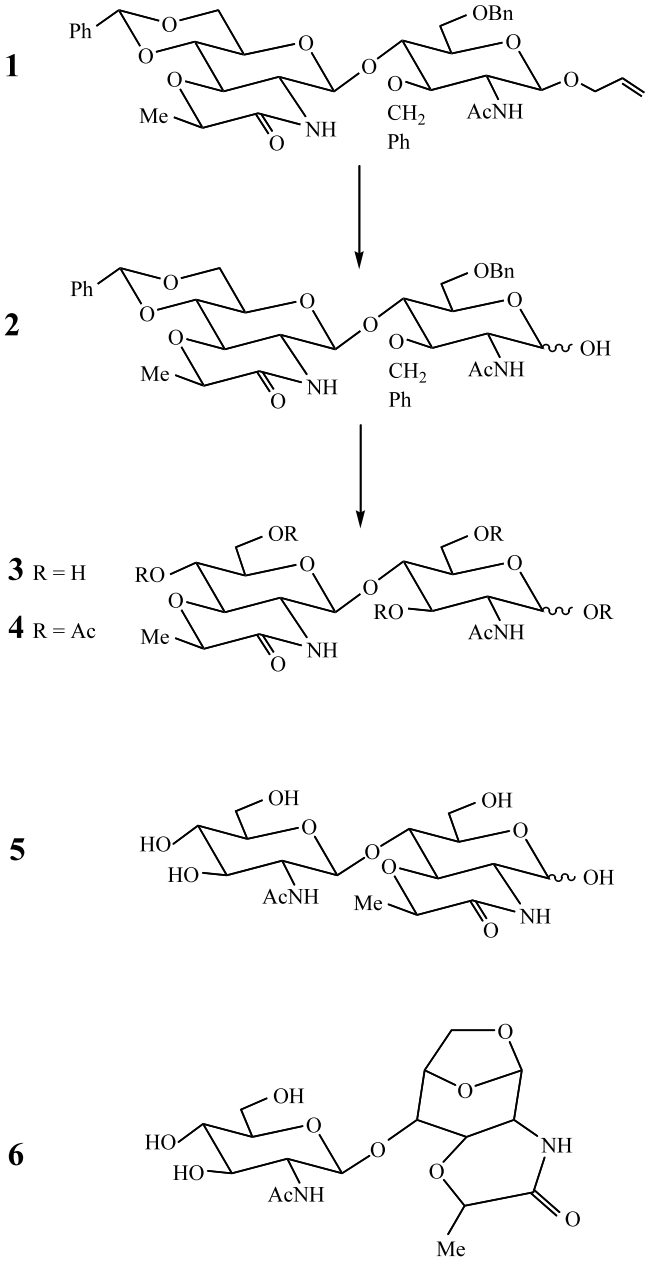

Scheme 1. Chemical formula of the compounds described in the paper.

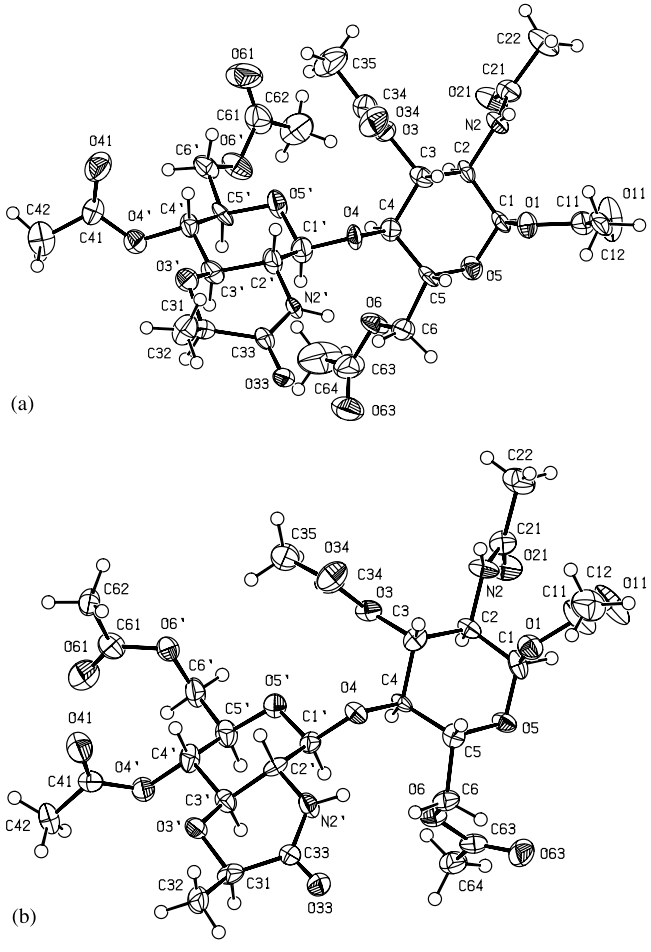

Fig. 1. ORTEP (Johnson, 1976) plot of two independent molecules **A** and **B** with the atom numbering. Thermal elipsoids are scaled the 30% probability level.

Table 1
^{1}H and ^{13}C chemical shifts, coupling constants in Hz (given in parenthesis) of per-*O*-acetylated disaccharide **4**

Sugar residue (position of *O*-acetyl)	H-1	H-2	H-3	H-4	H-5	H-6a	H-6b
	$J_{1,2}$	$J_{2,3}$	$J_{3,4}$	$J_{4,5}$	$J_{5,6a}$	$J_{5,6b}$	$J_{6a,6b}$
β-Mur-lactam-	4.42 d (8.0)	3.33 t (9.7)	3.59 t (9.7)	5.10 dd (9.6)	3.64 m (4.8)	4.34 dd (2.2)	4.06 dd (12.4)
(1→ (4-,6-) α	6.12 d (3.6)	4.41 m (10.9)	5.24 dd (9.3)	3.89 t (9.9)	3.97 m (2.2)	4.37 dd (4.8)	4.24 dd (12.4)
→4)-D-GlcNAc β (1-,3-,6-)	5.65 d (8.6)	4.27 m (9.7)	5.08 dd (9.7)	3.83 t (9.7)	3.82 m (2)	4.46 dd (4.8)	4.19 dd (12.2)
	C-1	C-2	C-3	C-4	C-5	C-6	
β-Mur Lactam (1→ (4-,6-) α	99.8	56.6	75.6	66.9	73.4	61.8	
→4)-D-GlcNAc(1-,3-,6-) β	90.5	50.8	70.5 [b]	74.2	70.6 [b]	61.9	
	92.5	52.6	72.1	74.5	74.0	62.3	

[a] Values obtained for solutions in $CDCl_3$ (internal Me_4Si).
[b] Signals for which assignement may be interchanged.

2.2. X-ray structure of 4

Crystals obtained after several months from a chloroform solution of **4** include two solvent molecules per asymmetric unit. In the unit cell there are two crystallographically independent molecules **A** and **B** (Fig. 1) that reveal some conformational differences (Fig. 2). The conformations of the acetamido groups of GlcNAc residues in molecules **A** and **B** are different. Among four theoretically possible conformations (defined with respect to the bonds C-2–N and N–C) two of them were observed: (*Z*)-syn (**A**) and (*Z*)-anti (**B**).[7] Both molecules, **A** and **B** are α-anomers (GlcNAc moiety) although in solution NMR data revealed an anomeric mixture (α:β = 3:1). The selected torsional angles describe the glucopyranose rings and δ-lactam ring conformations, and the conformation about glycosidic bonds (Table 2). The ring conformations are assigned according to the asymmetry parameters[8] and Cremer-Pople[9] values listed in Table 3. The complex system of hydrogen bonding is illustrated in Fig. 3 and geometrical parameters are listed in Table 4.

The D-glucopyranose moieties of GlcNAc and MurLac residues of the molecules **A** and **B** are in the chair $^{4}C_1$ conformation (Tables 2 and 3); distortion from ideal chair conformation in the MurLac residues is influenced by a fused δ-lactam ring and therefore their β-D-glucopyranose rings are more puckered (average torsion angle values are 60.6 and 61.2°, respectively). δ-Lactam ring of **B** is in a half-chair conformation with O-3′ and C-3′ displaced from the four atom plane by 0.154 and −0.615 Å, respectively. However, in molecule **A** a form between an envelope and the half-chair was observed (Table 3).

In the crystal packing the two-dimensional network in the (*ab*) plane (Table 4, Fig. 3) is realised by hydrogen bonds N–H···O between molecules **A** and **B**. How-

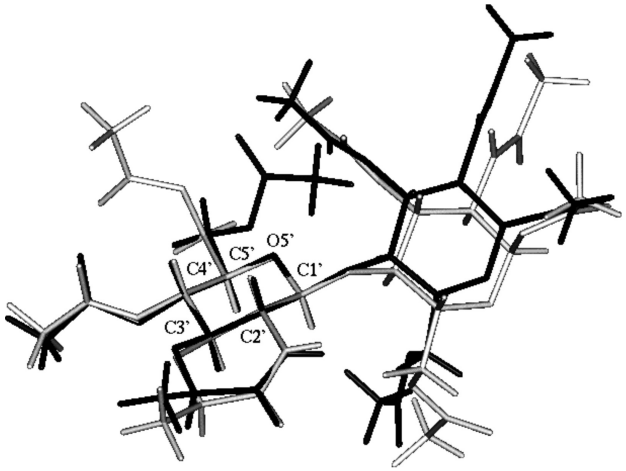

Fig. 2. Superposition diagram of the molecules **A** and **B** to show conformational diffrences. The labelled aoms were used for overlapping.

Table 2
Selected torsion angles (°) for **4**

	Molecule **A**	Molecule **B**		Molecule **A**	Molecule **B**
D-Glucopyranose of GlcNAc moiety			δ-Lactam ring		
O-5–C-1–C-2–C-3	57.1(10)	52.8(11)	N-2′–C-2′–C-3′–O-3′	60.6(10)	51.7(10)
C-1–C-2–C-3–C-4	−53.9(10)	−51.5(9)	C-2′–C-3′–O-3′–C-31	−69.5(9)	−72.1(9)
C-2–C-3–C-4–C-5	54.7(11)	52.2(9)	C-3′–O-3′–C-31–C-33	44.1(10)	54.0(9)
C-3–C-4–C-5–O-5	−55.4(11)	−54.7(9)	O-3′–C-31–C-33–N-2′	−11.4(12)	−19.0(11)
C-4–C-5–O-5–C-1	58.1(10)	57.3(9)	C-31–C-33–N-2′–C-2′	7.1(13)	2.0(13)
C-5–O-5–C-1–C-2	−58.7(10)	−55.1(10)	C-33–N-2′–C-2′–C-3′	−30.7(12)	−17.5(12)
D-Glucopyranose of MurLac moiety			Glycosidic bond		
O-5′–C-1′–C-2′–C-3′	60.3(10)	61.6(9)	O-5′–C-1′–O-4–C-4 (Φ)	−70.1(10)	−80.4(8)
C-1′–C-2′–C-3′–C-4′	−56.6(10)	−62.4(9)	C-1′–O-4–C-4–C-3 (Ψ)	131.7(8)	126.2(7)
C-2′–C-3′–C-4′–C-5′	55.8(11)	60.8(10)			
C-3′–C-4′–C-5′–O-5′	−58.3(10)	−59.7(10)			
C-4′–C-5′–O-5′–C-1′	65.0(10)	61.0(10)			
C-5′–O-5′–C-1′–C-2′	−66.6(10)	−61.1(9)			

Table 3
Asymmetry parameters and Cremer-Pople puckering parameters for **4**

Ring residue	Asymmetry parameters (°)	Cremer-Pople parameters	$w\langle\lvert$t.a.$\rvert\rangle$ (°)	Conformation
D-Glucopyranose of GlnNAc				
Mol **A**	ΔC_S(O-5) = ΔC_S(C-3) = 1.1 (9) ΔC_2(O-5–C-5) = ΔC_2(C-2–C-3) = 1.3 (10)	Q = 0.564(10) Å Θ = 0.0(9)° Φ = 189(35)°	56.4	α-$^4C_1$ = $^OC_3$ chair
Mol **B**	ΔC_S(O-5) = ΔC_S(C-3) = 1.7 (8) ΔC_2(C-2–C-3) = ΔC_2(C-5–O-5) = 0.5 (10)	Q = 0.535(10) Å Θ = 3.2(10)° Φ = 264(15)°	54.0	α-$^4C_1$ = $^OC_3$ chair
D-Glucopyranose of MurLac				
Mol **A**	ΔC_S(O-5′) = ΔC_S(C-3′) = 1.5 (8) ΔC_2(O-5′–C-1′) = ΔC_2(C-3′–C-4′) = 3.5 (10)	Q = 0.615(10) Å Θ = 3.5(9)° Φ = 31(17)°	60.6	β-$^4C_1$ = $^OC_3$ chair
Mol **B**	ΔC_S(C-2′) = ΔC_S(C-5′) = 0.9 (8) ΔC_2(C-1′–C-2′) = ΔC_2(C-4′–C-5′) = 0.9 (9)	Q = 0.624(10) Å Θ = 4.9(8)° Φ = 169(11)°	61.2	β-$^4C_1$ = $^OC_3$ chair
δ-Lactam ring				
Mol **A**	ΔC_S(C-3′) = ΔC_S(C-33) = 9.6 ΔC_2(O-3′–C-3′) = ΔC_2(N-2′–C-33) = 18.0	Q = 0.535(10) Å Θ = 47.4(11)° Φ = 52.0(14)°	42.9	$E_{C3'}/^{O3'}H_{C3'}$ envelope/half chair
Mol **B**	ΔC_S(O-3′) = ΔC_S(N-2′) = 23.4 ΔC_2(O-3′–C-3′) = ΔC_2(N-2′–C-33) = 1.9(10)	Q = 0.531(9) Å Θ = 48.6(10)° Φ = 30.6(14)°	42.4	$^{O3'}H_{C3'}$ half chair

Table 4
Hydrogen bond geometry for **4**

*D*onor-H···*A*cceptor	*D*–H (Å)	H···*A* (Å)	*D*···*A* (Å)	*D*–H···*A* (°)
A N-2′–H-21′···O-33^{i} **B**	0.86	2.086	2.929	167
A N-2–H-21···O-21^{ii} **B**	0.86	2.010	2.837	161
B N-2–H-21···O-21^{iii} **A**	0.86	1.999	2.809	157
B N-2′–H-22′···O-33^{iv} **A**	0.86	2.022	2.871	169

Symmetry operation on the donor atom: (i) $x, 1+y, z$; (ii) $1/2+x, 3/2+y, z$; (iii) $-1/2+x, -1/2+y, z$; (iv) $x, -1+y, z$.

ever, there are no hydrogen bonds between **A**···**A** nor **B**···**B**. Each molecule **A** is hydrogen bonded to three **B** and vice versa. Molecules **A** and **B**, each related by translation along axis *b*, form zig-zag chains through hydrogen bonds N-2–H···O21 of GlcNAc residues. Hydrogen bonds N-2′–H···O33 between MurLac residues connect molecule **A** from one chain to molecule **B** from the other chain (dimers **AB**) into direction of the *a* axis.

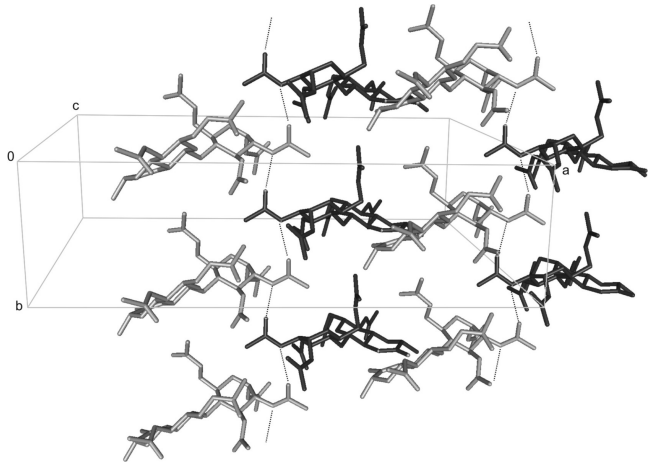

Fig. 3. Crystal packing diagram of **4** in the (*ab*) plane illustrates an infinite two dimensional hydrogen bond network. Each molecule **A** is hydrogen bonded to three molecules **B** and vice versa; N–H···O hydrogen bonds act between muramyl lactam residue of **A** to its analogue of **B**, and *N*-acetyl-glucosamine moieties of **A** and **B** are hydrogen bonded as well.

2.3. Molecular modelling

Conformational analysis is based on molecular modelling data by molecular mechanics and dynamics. In our previous papers we studied in detail the conformation of ring moieties in monosacharide derivatives of spore cortex units by X-ray structure analysis, NMR and molecular mechanics and dynamics.[2,3] In the disaccharides **3** and **5** studied in this paper molecular dynamics simulations showed that GlcNAc residue adopts predominantly the usual chair $^{4}C_{1}$ (i.e., $^{O}C_{3}$) conformation as well as glucopyranose ring of MurLac residue. The appearance of some other energetically less favourable conformations were observed during MD simulations at higher temperatures. δ-Lactam ring of MurLac residue showed to be in the sofa E_3 conformation during MD simulations, sometimes distorted towards the half-chair $^{O}H_3$ conformation. These results are in accordance with our previous studies on monosaccharides.[2,3] Here we are focused on the conformation around the glycosidic bond. Since the molecular mechanics and dynamics results are force field dependent two different approaches were used. Molecular mechanics geometry minimisations were performed using MM3(92)[10,11] and DISCOVER cvff.[12] Simultaneous systematic roatations of torsion angles around glycosidic bond O-5′–C-1′–O-4–C-4 (Φ) and C-1′–O-4–C-4–C-3 (Ψ) were preformed using MMSQ[13,14] program based on MM3(92) driver option and also in DISCOVER using cvff. A prudent-ascent algorithm in MMSQ program ensures that those conformations of the exocyclic groups are found to yield the lowest energy at each (Φ, Ψ). DISCOVER cvff was used for MD simulations. The results obtained were compared and correlated to the previously obtained modelling results for GlcNAc-1,6-anhydro-MurLac (**6**) based on the X-ray structure as an initial model.[3]

For disaccharide GlcNAc-MurLac (**5**) both simulations with MMSQ and DISCOVER were performed. Local minima at the two-dimensional contour map of energy surface for simultaneous rotation of Φ and Ψ in MMSQ are overlapped by the populated torsion angles from the MD simulation (DISCOVER) (Fig. 4). MMSQ map reveals four distinctive energy minima (Φ, Ψ) around (-75, 115°), (-115, 75°), (-85, -75°) and (55, 125°) that are also populated in MD simulations. The energy difference between the four optimal conformers is within 1 kcal mol^{-1}. The first two minima together with energetically less favoured ($\Delta E < 3$ kcal mol^{-1}) fifth minimum, (Φ, Ψ) around (-55, 175°), can be considered as a part of one wide minimum. Minimisation of conformers sampled from MD trajectories revealed several stable conformations close to the above stated minima. The simultaneous rotation

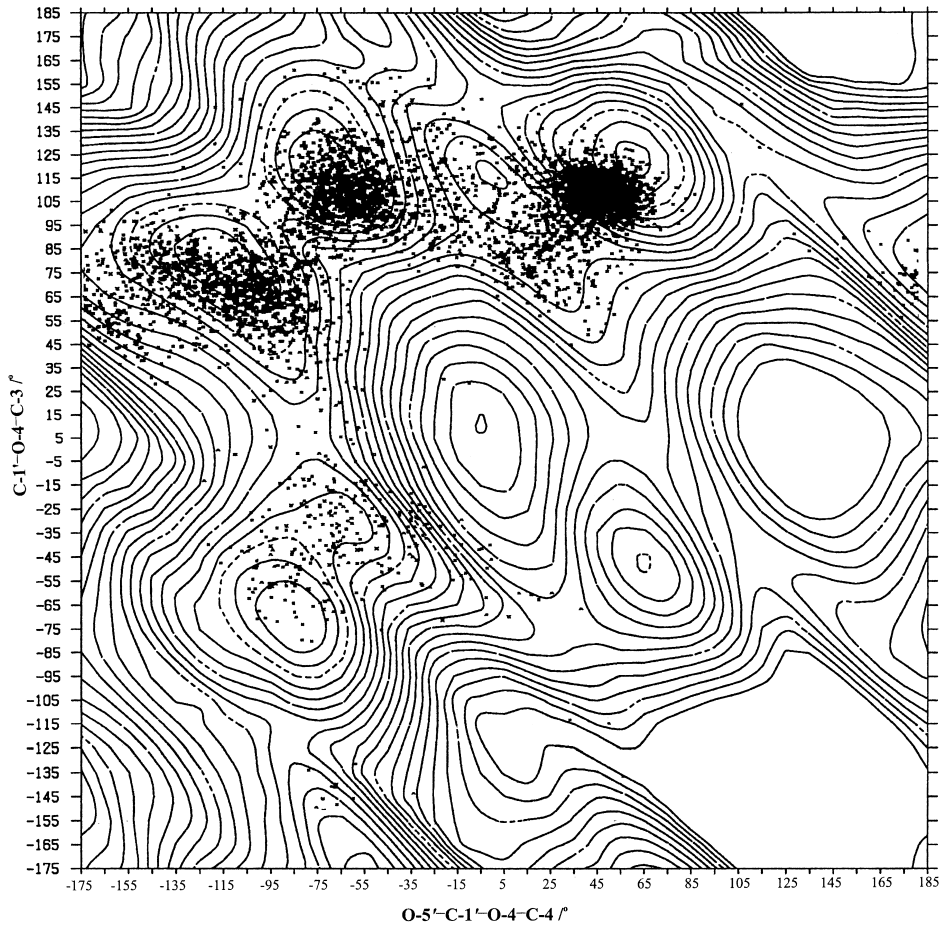

Fig. 4. Two-dimensional energy surface diagram (kcal mol^{-1}) with a separation energy levels of 1 kcal mol^{-1} as a function of two torsional angles Φ and Ψ for **5** (obtained by program MMSQ[14]) with superimposed results obtained by molecular dynamics simulations representing population of particular values of torsion angles defining conformation about the glycosidic bond.

around glycosidic bond in DISCOVER using cvff gave similar results.

The conformational profile for GlcNAc-MurLac (**5**) (Fig. 4) showed to be similar to the profile for the disaccharide GlcNAc-1,6-anhydro-MurLac (**6**) (Fig. 5) studied earlier.[3] In MMSQ contour map four minima (Φ, Ψ) around (-85, 145°) and (-105, 75°) (these two can be considered as one broad minimum) and (-95, -75°), (65, 135°) were located. They were also found to be populated during the DISCOVER MD simulations [(-76, 154°), (-94, 69°) and (50, 125°)]. The local minima of (Φ, Ψ) in (+)-synclinal, (+)-anticlinal range detected by MD simulations, recognised also by MMSQ, are highly populated. The X-ray conformation observed for GlcNAc-1,6-anhydro-MurLac with (Φ, Ψ) (-99, 76°)[3] falls within the second minimum stated above. It can be concluded that closure of 1,6-anhydro ring at the cortex terminus does not affect the conformation around glycosidic bond.

The results obtained for GlcNAc-MurLac and GlcNAc-1,6-anhydro-MurLac with different methods (molecular modelling and X-ray analysis), different simulation protocols (MM, MD, dihedral driver) and different force fields (MM3(92) and cvff in DISCOVER) agreed well. Therefore the conformational analysis of MurLac-GlcNAc disaccharide (**3**) was performed by DISCOVER, only. MD simulations for **3** revealed populated minima around (Φ, Ψ) (-90, 120°) (-100, 70°) and (50, 120°) (Fig. 6). However, minimum around (Φ, Ψ) (-90, -75°) detected as low populated for compounds **5** and **6**, is not populated for **3** at all. The dihedral driver option performed within DISCOVER (cvff) gave the same results.

The numerical methods used for conformational analysis gave consistent results. All of them recognised the low energy glycosidic conformations: (−)-synclinal, (+)-anticlinal; (−)-anticlinal, (+)-synclinal; (−)-synclinal, (−)-synclinal, and (+)-synclinal, (+)-anticlinal.[15] In all three disaccharides studied the first two minima [(Φ, Ψ) around (-90, -75°) and (-110, 75°)] with hardly any barrier between them, can be considered as one broad minimum with considerable flexibility. Conformational freedom in the region 3 [(Φ, Ψ) around (-90, -75°)] is much more restricted and

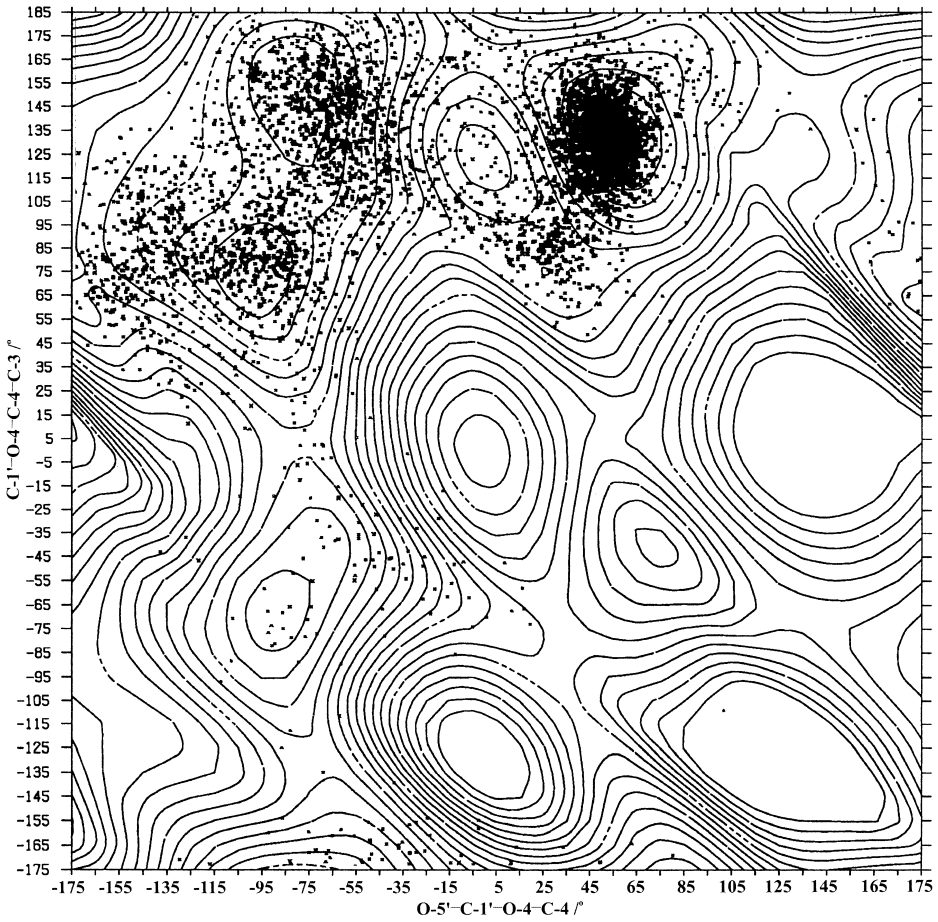

Fig. 5. Two-dimensional energy surface diagram (kcal mol^{-1}) with a separation energy levels of 1 kcal mol^{-1} as a function of two torsional angles Φ and Ψ for **6** (obtained by program MMSQ[14]) with superimposed results obtained by molecular dynamics simulations representing population of particular values of torsion angles defining conformation about the glycosidic bond.

this region appears to be separated from 1 by a large barrier. The route to region 4 [(Φ, Ψ) around (60, 125°)] stabilised by intramolecular hydrogen bonds, goes through a saddle point. The lower left quadrant in the conformational map (Figs. 4 and 5) is energetically unfavourable region with four local maxima and one saddle point between them. The X-ray glycosidic conformation of **4**, being peracteylated analogue of **3**, is (−)-synclinal, (+)-anticlinal whereas of 1,6-anhydro analogue **6** is (−)-anticlinal, (+)-synclinal. They both lie within the first two minima as we observed for the crystal structures of β-(1→4)-disaccharides found in the Cambridge Structural Database.[16] According to the analysis performed it can be seen that chemical modifications introduced have not restricted glycosidic bond flexibility. The data obtained suggest rather flexible glycosidic conformations as was already observed in other β-(1→4) disaccharides such as chitobiose[17] and cellobiose (molecular modelling supported by experimantal ROESY NMR data[18] and X-ray structure of α-cellobiose·2NaI·$2H_2O$ complex[19]). It is more likely

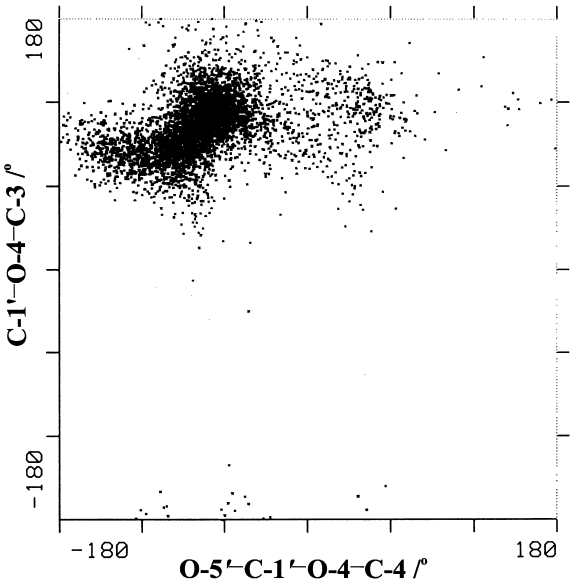

Fig. 6. The results of molecular dynamics simulations for **3** revealing population of conformers about glycosidic bond.

Table 5
Crystallographic data, structure solution and refinement of **4**

Compound	**4**
Empirical formula	$C_{27}H_{38}N_2O_{16}$, $CHCl_3$
M_r	765.96
Temperature (K)	100 (3)
Wavelength (Å)	1.54180
Crystal system	monoclinic
Space group	*C*2
a (Å)	32.604(5)
b (Å)	9.170(5)
c (Å)	25.351(5)
β (°)	94.906(5)
V (Å^3)	7552(5)
Z	8
D_x (Mgm^{-3})	1.347
Absorption correction	none
Total data collected	7654
Observed data [$I>2\sigma(I)$]	6831
Θ_{max}	50.09
Range of *h*,*k*,*l*	−31,31; −9,9; −25,25
R_1 [$F_o>4\sigma(F_o)$]	0.0884
wR_2 (F^2)	0.2254
S	1.050
Parameters	897
$\Delta\rho_{max}$, $\Delta\rho_{min}$ (e Å^{-3})	1.903, −0.515
Weighting scheme*	$w=1/[\sigma^2(F_o^2)+0.1916P^2+14.8746P]^*P=(F_o^2+2F_c^2)/3$

that flexibility of glycosidic bond is one of key parameters in molecular recognition processes and a degree of its rotational freedom can be related to the nature of a receptor and its function.

3. Experimental

3.1. General methods

Column chromatography was performed on silica gel (Merck 0.040–0.063 mm) and TLC on silica gel 60 with detection by charring with 10% H_2SO_4, chlorine–iodine reagent or ninhydrin. Optical rotations were determined with an Optical Activity LTD automatic AA-10 Polarimeter. NMR spectra were recorded with Varian Gemini 300 spectrometer and for compound **4** with Bruker Avance DRX 500 spectrometer. Spectra were recorded in $CDCl_3$, if not stated otherwise, with Me_4Si as the internal standard. Exchangeable protons were detected by addition of D_2O. The proton assignments are based on $^1H-^1H$ COSY measurements and for **4** on $^1H-^{13}C$ HETCOR measurements and HMQC and HMBC experiments.

3.2. *O*-(2-Amino-4,6-*O*-benzylidene-3-*O*-[(*R*)-1-carboxyethyl]-2-deoxy-β-D-glucopyranosyl-1′,2-lactam)-(1→4)-2-acetamido-3,6-di-*O*-benzyl-2-deoxy-D-glucopyranose (2)

To a solution of the allyl glycoside **1** (102 mg, 0.137 mmol) in 7:3:1 EtOH–toluene–water (25 mL) was added tris(triphenyl phosphine) rhodium(I) chloride (52.2 mg, 0.056 mmol) and 1,8-diazabicyclo[2.2.2]octane (Dabco, 32 mg, 0.285 mmol) and the mixture was stirred at 80 °C for 36 h (monitoring by TLC in 10:10:1 toluene–EtOAc–MeOH). The solvent was removed, the residue was dissolved in acetone (5 mL) containing mercuric oxide (2.5 mg, 0.0115 mmol) and to this mercuric chloride (222.3 mg, 0.82 mmol) was added in 9:1 acetone–water (10 mL) and the mixture was stirred for 2 h at room temperature (rt). Following evaporation, the residue was extracted with $CHCl_3$ and the combined extracts were washed with 30% KI followed by water and dried (Na_2SO_4). Evaporation left a syrup which was purified by column chromatography with 5:5:1 toluene–EtOAc–MeOH to give an anomeric mixture of **2** (82 mg, 85%) as an amorphous mass. ^1H NMR ($CDCl_3$): δ 7.6–7.3 (m, 15 H, 3 × Ph), 6.46 (bs, 1 H, disappeared on H–D exchange, N*H*′), 5.70 (d, $J_{NH,2}$ 9 Hz, disappeared on H–D exchange, N*H*), 5.46 (s, 1 H, PhC*H*), 5.20 (m, ~0.7 H, on H–D exchange changed to 5.17 d, $J_{1,2}$ 3.59 Hz, H-1α), 4.80, 4.75, 4.56, 4.48 (4 d, 4 H, *J* 12 Hz, 2 × PhCH_2), 4.79 (d, ~0.3 H, $J_{1,2}$ 8.2 Hz, H-1β), 4.41 (d, 1 H, $J_{1,2}$, 8.1 Hz, H-1′), 4.34–4.0 (m, ~4 H, H-2, H-6a, H-6′a, α-C*H* Lact), 4.08 (t, $J_{4,3}$ 9.2, $J_{4,5}$ 9.7, H-4), 3.95–3.40 (m, H-3, H-6b, H-4′, H-6′b), 3.46 (t, 1 H, $J_{3,2}$ 9.5, $J_{3,4}$ 9.2 Hz, H-3′) 3.30–3.15 (m, H-5, H-5′), 3.26 (t, 1 H, H-2′), 1.85 (s, NAc), 1.49 (d, 3 H, $J_{Me,CH}$ 6.7 Hz, Me-Lact). Anal. Calcd for $C_{38}H_{44}N_2O_{11}$: C, 64.76; H, 6.29; N, 3.97. Found: C, 64.69; H, 6.31; N, 4.00.

4. *O*-(2-Amino-3-*O*-[(*R*)-1-carboxyethyl]-2-deoxy-β-D-glucopyranosyl-1′,2-lactam)-(1→4)-2-acetamido-2-deoxy-D-glucopyranose (3)

Compound **2** (101 mg, 0.143 mmol) was dissolved in 9:1 MeOH–AcOH (12 mL) containing 10% Pd/C (125 mg) and the mixture was stirred under hydrogen for 48 h at rt. Catalyst was removed by filtration over Celite and the filtrate was evaporated and co-evaporated with toluene to give **3** (45 mg, 72%) as an amorphous mass $[\alpha_D]$ +4° (*c* 1, MeOH). ^1H NMR (D_2O): δ 5.07 (d, ~0.7 H, $J_{1,2}$ 1.9 Hz, H-1α), 4.81 (d, ~0.3 H, $J_{1,2}$ 8.1 Hz, H-1β), 4.61 (d, 1 H, $J_{1,2}$ 8.1 Hz, H-1′), 4.29 (q, $J_{CH,Me}$ 6.8 Hz, α-C*H*-Lact), 3.92–3.61 (m, 7 H, H-2, H-3, H-5, H-6a, H-6b, H-6′a, H-6′b), 3.88 (t, $J_{3,2}$ 9.8, $J_{3,4}$ 9.1 Hz, H-3), 3.60 (dd, $J_{3,4}$ 9.1, $J_{4,5}$ 9.8 Hz, H-4), 3.54 (t $J_{4,3}$ 9.3, $J_{4,5}$ 9.1 Hz, H-4′), 3.47 (t, $J_{3,2}$ 9.3, $J_{3,4}$ 8.9

Hz, H-3′) 3.45–3.30 (m, $J_{5,6a}$, 2 Hz, $J_{5,6b}$ 5Hz, H-5′), 3.26 (t, H-2′), 1.92 (s, N*Ac*), 1.35 (d, 3 H, $J_{Me,CH}$ 6.8 Hz, Me-Lact). Anal. Calcd for $C_{17}H_{28}N_2O_{11}$: C, 46.78; H, 6.47; N, 6.42. Found: C, 46.52; H, 6.69; N, 6.32.

4.1. *O*-(4,6-Di-*O*-acetyl-2-amino-3-*O*-[(*R*)-1-carboxyethyl]-2-deoxy-β-D-glucopyranosyl 1′,2-lactam)-(1→4)-2-acetamido-1,3,6-tri-*O*-acetyl-2-deoxy-D-glucopyranose (4)

Compound **3** (30 mg, 0.069 mmol) was dissolved in 1:1 Ac_2O–Py (2.0 mL) and stirred for 24 h at rt. The solvent was evaporated and the residual volatiles co-evaporated with toluene–EtOH (4 ×). The residue was chromatographed on a SiO_2 column using 8:1 EtOAc–propan-2-ol to give anomeric **4** (33 mg, 74%) as an amorphous mass. ^{1}H NMR ($CDCl_3$ 500 MHz): δ 6.60 (bs, 1 H, N*H*′), 5.76 (d, $J_{NH,2}$ 9.3 Hz, N*H* GlcNAc-β), 5.57 (d, $J_{NH,2}$ 9.1 Hz, N*H* GlcNAc-α), 4.23 (q, $J_{CH,Me}$ 6.8 Hz, α-C*H* Lact), 2.188, 2.151, 2.109, 2.087, 2.077, 2.065 (6 s, 15 H, OAc), 1.944 (s, NAc of GlcNAc-α), 1.936 (s, NAc of GlcNAc-β), 1.45 (d, 3 H, $J_{Me,CH}$ 6.8 Hz, Me Lact); ^{13}C NMR (125 MHz): δ 171.5 (*C*O Lactam), 171.4, 170.7, 170.5, 170.1, 169.5, 168.7 (*C*O Ac), 75.0 (α-*C*H Lact), 23.2 (*Me* of GlcNAc-β), 23.1 (*Me* of GlcNAc-α), 20.9, 20.88, 20.78, 20.70, 20.67, 20.59 (*Me* Ac), 17.5 (*Me* Lact). Other NMR data are given in Table 1. Anal. Calcd for $C_{27}H_{38}N_2O_{16}$: C, 50.15, H, 5.92; N, 4.33. Found: C, 49.90; H, 6.02; N, 4.20.

4.2. X-ray structure determination of 4

The crystals for X-ray structure analysis were obtained from chloroform at rt. The crystal data and summary of experimental details are listed in Table 5. The X-ray intensity data were collected with a Bruker–Nonius Kappa CCD area-detector diffractometer supplied by a rotating anode tube and Cu K_α radiation using COLLECT.[20] Data reduction was by DENZO and SCALEPACK[21] The structure was solved by SIR-97[22] and refined on F^2 by SHELXL-97.[23] Details of the refinement are given in Table 5. During the structure determination, the D-enantiomer was selected according to the assignment *R* at C-5; chirality on C-31 (δ-lactam residue) proved to be *R*. The molecular geometry was calculated by program PLATON[24] and the molecular structure presented by ORTEP.[25]

4.3. Conformational analysis

Molecular dynamics (MD) calculations were carried out with the program DISCOVER[12] using the consistent valence force field (cvff) based on Lifson and Warshel[26] and Hagler and co-workers[27,28] at temperature of 300 K which was gradually elevated to 1200 K in order to enable possible conformational changes during 500 ps. Different conformations obtained in this way were energy minimised by molecular mechanics in DISCOVER. The starting geometries were generated in the BUILDER module of INSIGHTII[29] using the X-ray data as model and energy minimised in DISCOVER (cvff) prior to starting MD. Since bacterial spore represents dormant stage of life which almost excludes the simulations in water simulations in water were not of biological interest. All simulations were performed in vacuo ($\varepsilon_r = 1.0$).

Conformational space was searched also using the dihedral driver option in DISCOVER for the angles around the glycosidic bond, O-5′–C-1′–O-4–C-4 (Φ) and C-1′–O-4–C-4–C-3 (Ψ). Rotation in 10° increments was performed without subsequent geometry optimisation and with geometry optimisation using the force of 100 kcal rad^{-2}. The same energy maps were calculated also using another force field and program—MM3(92).[11] To obtain the minimum of other degrees of freedom (e.g., hydroxyl group orientations) at each (Φ, Ψ) the method of prudent ascent[13] was used. It involves the use of completely automated procedure[14] as an interface to the MM3(92) driver option. This method leads to a smooth energy profile when driving two torsion angles. For calculations with MMSQ[14] the starting geometries were first energy minimised with MM3(92). Dielectric constant of 1.5 was used.

All calculations were performed on OCTANE, Silicon Graphics workstation of the Laboratory for Chemical and Biological Crystallography of the Rudjer Bošković Institute, Zagreb, Croatia.

5. Supplementary material

Crystallographic data on the structure have been deposited at the Cambridge Crystallographic Data Centre, CCDC No. 185529 for compound **4**. Copies of this information may be obtained free of charge from The Director, CCDC, 12 Union Road, Cambridge, CB2 1EZ, UK (Fax: +44-1223-336-033; e-mail: deposit@ccdc.cam.ac.uk or www: http://www.ccdc.cam.ac.uk. The atom numbering in the paper is in accord with IUPB rules whereas in deposited material it satisfies the CIF format.

Acknowledgements

This work was supported by Ministry of Science and Technology of Republic of Croatia grants 0098054 and 0098036. The authors thank Dr Loes Kroon-Batenburg, Department of Crystal and Structural Chemistry, Bijvoet Center for Biomolecular Research,

Rijksuniversiteit Utrecht, The Netherlands for her valuable help and comments on confomation analysis, and Biserka Metelko, PLIVA, for crystallisation of the compound **4**.

References

1. Moir, A.; Smith, D. A. *Annu. Rev. Microbiol.* **1990**, *44*, 531–553.
2. Keglević, D.; Kojić-Prodić, B.; Banić, Z.; Tomić, S.; Puntarec, V. *Carbohydr. Res.* **1993**, *241*, 131–152.
3. Banić, Z.; Kojić-Prodić, B.; Kroon-Batenbourg, L.; Keglević, D. *Carbohydr. Res.* **1994**, *259*, 159–174.
4. Keglević, D.; Kojić-Prodić, B.; Banić Tomišić, Z.; Spek, A. L. *Carbohydr. Res.* **1998**, *313*, 1–14.
5. Gigg, R.; Warren, C. D. *J. Chem. Soc. Sect. C* **1968**, 1903–1911.
6. Kanie, O.; Crawley, S. C.; Palcic, M. M.; Hindsgaul, O. *Carbohydr. Res.* **1993**, *243*, 139–164.
7. Mazeau, K.; Pérez, S.; Rinaudo, M. *J. Carbohydr. Chem.* **2000**, *19*, 1269–1284.
8. Duax, W. L.; Weeks, C. M.; Rohrer, D. C. *Top. Stereochem.* **1974**, *9*, 283–383.
9. Cremer, D.; Pople, J. A. *J. Am. Chem. Soc.* **1975**, *97*, 1354–1367.
10. Allinger, N. L.; Rahman, M.; Lii, J. H. *J. Am. Chem. Soc.* **1990**, *112*, 8293–8307.
11. Allinger, N.L. The program MM3 (92) is obtained via the Technical Utilization Corporation, Powell, Ohio, USA.
12. DISCOVER, version 2.9.7 BIOSYM Technologies, San Diego, CA, USA, 1995.
13. Hooft, R. W. W.; Kanters, J. A.; Kroon, J. *J. Comput. Chem.* **1991**, *12*, 943–947.
14. Hooft, R.W.W. Quantum Chemistry Program Exchange no. 623, Chemistry Department, Indiana University, IN, USA 1993.
15. Klyne, W.; Prelog, V. *Experientia* **1960**, *16*, 521–523.
16. Allen, F. H.; Kennard, O. *Chem. Automat. News* **1993**, *8* (1), 31–37.
17. Espinosa, J.-F.; Asensio, J. L.; Bruix, M.; Jimenes-Barbero, J. *Anal. Quim. Int. Ed.* **1996**, *92*, 320–324.
18. Kroon-Batenburg, L. M. J.; Kroon, J.; Leeflang, B. R.; Vliegenhart, J. F. G. *Carbohydr. Res.* **1993**, *245*, 21–42.
19. Peralta-Inga, Z.; Johnson, G. P.; Dowd, M. K.; Rendleman, J. A.; Stevens, E. D.; French, A. D. *Carbohydr. Res.* **2002**, *337*, 851–861.
20. Nonius, COLLECT, Nonius BV, Delft, The Netherlands, 2000.
21. Otwinowski, O.; Minor, W. Methods in Enzymology. In *Macromolecular Crystallography*, *Part A*; Carter, C. V.; Sweet, R. M., Eds.; Academic Press: London, 1997; Vol. 276, pp 307–326.
22. Altomare, A.; Burla, M. C.; Camalli, M.; Cascarano, G.; Giaccovazzo, C.; Guagliardi, A.; Moliterni, A. G. G.; Polidori, G.; Spagna, R. *J Appl. Cryst.* **1999**, *32*, 115–119.
23. Sheldrick, G.M., SHELXL-97 Programs for Crystal Structure Analysis, 1998.
24. Spek, A.L. PLATON-98, A Multipurpose Crystallographic Tool, 120398 Version, University of Utrecht, Utrecht, The Netherlands, 1998.
25. Johnson, A.K. ORTEPII, Report ORNL-5138, Oak Ridge National Laboratory, Tennessee, USA, 1976.
26. Lifson, S.; Warschel, A. *J. Chem. Phys.* **1969**, *49*, 5116–5327.
27. Hagler, A. T.; Huler, Z.; Lifson, S. *J. Am. Chem. Soc.* **1974**, *98*, 5319–5327.
28. Hagler, A. T.; Lifson, S.; Dauber, P. *J. Am. Chem. Soc.* **1979**, *101*, 5122–5130.
29. INSIGHTII, release 95.0, BIOSYM Technologies, San Diego, CA, USA, 1995.